Preprints of the 19th World Congress
The International Federation of Automatic Control
Cape Town, South Africa. August 24-29, 2014

Advanced Control Education: Optimal & Robust MIMO Control of a Flexible Beam Setup

Christian Dullinger * **Alexander Schirrer** * **Martin Kozek** *

* *Vienna University of Technology, Austria (e-mail: christian.dullinger@tuwien.ac.at).*

Abstract: This paper discusses and illustrates core aspects in control education (prerequisites, working conditions, course structure) necessary to empower students of general engineering disciplines to understand and apply advanced optimal and robust control concepts. The results of a master thesis on the robust and optimal control of a flexible beam laboratory setup are presented and related to the skills formed during the undergraduate studies. Optimal and robust control design methods are utilized for active damping of bending vibrations of a simply supported thin structural aluminium beam. For this purpose a multi-input multi-output (MIMO) control system setup is used, comprising four collocated piezo patch actuators and sensors acting in longitudinal direction. An electrodynamic shaker introduces a disturbance force in the direction of oscillation. The design plant is obtained by a measurement-data-driven system identification. Also, finite element based modelling is carried out. The suitability of Linear-Quadratic Gaussian (LQG) control with modal weighting, mixed-sensitivity $\mathcal{H}_\infty$ control and D(G)K-synthesized control for improving disturbance rejection of the experimental control system setup is investigated and compared.

Keywords: Advanced Control Education; Vibration Control; Robust Control; Application of Mechatronic Principles

1. INTRODUCTION

Control education is an integral part of electrical and mechanical engineering studies. Mandatory courses typically cover fundamentals like transfer functions, stability, and controller design for linear single-input single-output (SISO) systems. In some curricula courses on the basics of state-space methods and multi-input multi-output (MIMO) systems are also mandatory. However, specific courses for advanced control methods such as $\mathcal{H}_\infty$-control cannot be offered as mandatory courses in a general engineering curriculum. This paper presents the results of a master's thesis in mechanical engineering (Dullinger, 2013) and focuses on the educational framework necessary to achieve such results.

At Vienna University of Technology (VUT) the curricula for bachelor and master studies in mechanical engineering each feature only one mandatory control education lecture and the associated control lab, see VUT (2011). In order to enable students to successfully implement advanced control concepts such as $\mathcal{H}_\infty$-control several necessary conditions must be fulfilled:

- a sound foundation in basic sciences (primarily mathematics)
- availability of elective courses in control engineering (preferably offering some flexibility with regards to content)
- tried and tested experimental setups for implementation (to minimize implementation overhead)

At VUT the first condition is fulfilled by three consecutive extensive mathematics courses with exercises, followed by two courses focusing on numerical engineering mathematics and stochastics. The importance of ordinary differential equations, the notion of stability, but also of linear algebra as core parts must be stressed here, see Kheir et al. (1996). Additionally, courses on mechanics, fluid dynamics, electrical and electronic systems, and thermodynamics complete the foundation of basic sciences during the bachelor studies.

The second condition is fulfilled by a variety of more advanced control courses, however, no specific course for $\mathcal{H}_\infty$-control is currently being offered. This is compensated by a seminar, an individually designed control project, and an advanced control lab. These three courses enable a flexible control education tailored for a specific implementation goal. In the case of the work presented here, no custom software tool was used although a variety of such tools exist: Senol et al. (2012); Ye et al. (2009); Kozek et al. (1999); instead, standard textbooks for $\mathcal{H}_\infty$-control provided the subject background (Skogestad and Postlethwaite, 2005).

Note that all knowledge on robust control has been acquired by the student during the master work.

The implementation of a closed-loop control together with experimental work is of especially high educational value, Kheir et al. (1996). On the one hand this poses a strong motivation to go through more theoretical and mathematical procedures without losing focus, on the other hand the students become familiar with many important aspects of real control implementations. In order to minimize the sometimes frustrating work of setting up the basic functionalities of the experimental setup, a tried and tested lab setup of a flexible beam with Piezo-patch sensors and actuators is utilized. Equally important is a user-friendly interface which allows for quick and easily verifiable implementation of the developed control algorithms.

In the remainder of this paper first the applied control designs are presented and the corresponding curricula requirements are outlined. Then the flexible beam laboratory setup is explained and the modelling task is briefly addressed. The subsequent sections summarize the specific control design tasks and the results of the experimental controller implementation, thereby demonstrating the outcome of the work.

2. MOTIVATION

Optimizing a construction for low weight generally leads to structures with decreased overall stiffness and lower natural frequencies of structure vibrations. Because of low damping, occurring vibrations can grow to large amplitudes. For these reasons, so-called "smart structures" are increasingly employed. Due to their properties, such as low weight, small dimensions, simple embeddability, efficiency, and longevity, piezo patches are well-suited as actuators and sensors for structural control applications. In this domain, novel so-called macro fiber composites (MFC) exhibit almost hysteresis-free, linear behaviour, see Smart Material (2013).

In this work, structural models were obtained from measurement data using a system identification method and also via the finite element (FE) method. Model mismatch – that is, differences between the actual system and the model of the system which was used to design the controller – were explicitly addressed in the controller design. A control system is said to be robust if (by design) it is insensitive to adequate definitions of model uncertainty.

As a simple tunable optimal design method, Linear-Quadratic Gaussian (LQG) control (Athans, 1971; Zhou et al., 1996) with modal weighting is well-suited to address the damping of undesirable eigenmodes. However, robustness can not directly be tuned or guaranteed, see Schirrer (2011). This directly motivates the application of optimal and robust $\mathcal{H}_\infty$ control design methods in structural control which do provide suitable robustness guarantees. The robust $\mathcal{H}_\infty$ control methods utilize frequency-dependent weights, and their performance heavily depends on an adequate uncertainty description. Mixed-sensitivity $\mathcal{H}_\infty$-optimal control has implicit robustness properties and is efficiently solvable in the standard framework of $\mathcal{H}_\infty$-(sub)-optimal control design. A more complex design method called D(G)K-iteration produces μ-"optimal" controllers and can exploit explicit uncertainty models in the process, making it potentially even more powerful. The quantity μ denotes the structured singular value. However, a D(G)K design requires significantly more tuning effort and often yields controllers of large dynamic order.

The aforementioned design methods are briefly reviewed and commented in the following section, see also Skogestad and Postlethwaite (2005).

3. DESIGN METHODOLOGY

3.1 Linear system representation

For linear systems the superposition principle

$$\boldsymbol{y}(s) = \boldsymbol{G}(s)\boldsymbol{u}(s) + \boldsymbol{G}_\mathrm{d}(s)\boldsymbol{d}(s) \tag{1}$$

holds, where $\boldsymbol{G}(s)$ and $\boldsymbol{G}_\mathrm{d}(s)$ are the transfer function matrices of the plant and the disturbance model, respectively. The vectors $\boldsymbol{y}$, $\boldsymbol{u}$ and $\boldsymbol{d}$ denote the outputs to be controlled, the control inputs, and the disturbance signals, respectively.

In the following let a minimal state-space representation of $[\,\boldsymbol{G}(s)|\boldsymbol{G}_\mathrm{d}(s)\,]$ be given by

$$\boldsymbol{G}(s) \overset{\mathrm{ss}}{=} \left[\begin{array}{c|c}\boldsymbol{A} & \boldsymbol{B}\\ \hline \boldsymbol{C} & \boldsymbol{D}\end{array}\right], \quad \boldsymbol{G}_\mathrm{d}(s) \overset{\mathrm{ss}}{=} \left[\begin{array}{c|c}\boldsymbol{A} & \boldsymbol{B}_\mathrm{d}\\ \hline \boldsymbol{C} & \boldsymbol{D}_\mathrm{d}\end{array}\right]. \tag{2}$$

3.2 Modally weighted LQG control

Linear Quadratic Gaussian (LQG) control assumes the plant dynamics be linear and known with stochastic noise excitation of known statistical properties,

$$\dot{\boldsymbol{x}} = \boldsymbol{A}\boldsymbol{x} + \boldsymbol{B}\boldsymbol{u} + \overline{\boldsymbol{w}} \tag{3}$$

$$\boldsymbol{y} = \boldsymbol{C}\boldsymbol{x} + \boldsymbol{D}\boldsymbol{u} + \overline{\boldsymbol{v}}, \tag{4}$$

where the process noise $\overline{\boldsymbol{w}}$ and measurement noise $\overline{\boldsymbol{v}}$ are usually assumed to be uncorrelated zero-mean Gaussian stochastic processes with known constant power spectral density matrices $\boldsymbol{W}$ and $\boldsymbol{V}$ respectively, see Skogestad and Postlethwaite (2005); Schirrer (2011).

Given the system (3)–(4) the LQG control problem is to find the optimal control $\boldsymbol{u}(t)$ which minimizes

$$J = \mathrm{E}\left\{\lim_{T\to\infty}\frac{1}{T}\int_0^T \left[\boldsymbol{x}(t)^\mathrm{T}\boldsymbol{Q}\boldsymbol{x}(t) + \boldsymbol{u}(t)^\mathrm{T}\boldsymbol{R}\boldsymbol{u}(t)\right]\mathrm{d}t\right\}, \tag{5}$$

where $\boldsymbol{Q} = \boldsymbol{Q}^\mathrm{T} \geq 0$ and $\boldsymbol{R} = \boldsymbol{R}^\mathrm{T} > 0$ are appropriately chosen constant real weighting matrices.

Due to the separation principle the solution of (5) can be decomposed into the finding of the Kalman filter – an optimal observer – and an optimal state feedback control gain.

Choosing $\boldsymbol{Q}$ as a modal weighting matrix is appropriate for cases in which certain undesirable eigenmodes of the plant $\boldsymbol{G}(s)$ shall be weighted directly. This is of special interest for active damping of flexible structures with low-damped modes, where each mode is excited almost independently and the total structural response is the sum of modal responses, see Gawronski (2004).

Let the columns of $\boldsymbol{S}$ consist of n linearly independent eigenvectors $\boldsymbol{s}_k$ (for $k = 1, \ldots, n$) of the state matrix $\boldsymbol{A}$ and $\boldsymbol{M}$ be a diagonal matrix of scalar weighting factors $m_k \geq 0$. Then, the state weighting matrix $\boldsymbol{Q}$ for modal weighting reads:

$$\boldsymbol{Q} = \widehat{\boldsymbol{Q}}^\mathrm{T}\widehat{\boldsymbol{Q}} \text{ with } \widehat{\boldsymbol{Q}} = \boldsymbol{S}\boldsymbol{M}\boldsymbol{S}^{-1} \tag{6}$$

Consequently, the kth eigenmode $\boldsymbol{s}_k$ is weighted by the value m_k^2, assuming that $\|\boldsymbol{s}_k\|_2 = 1$ holds.

Educational prerequisites for this design are linear algebra, basics of state feedback control, and a sound understand-

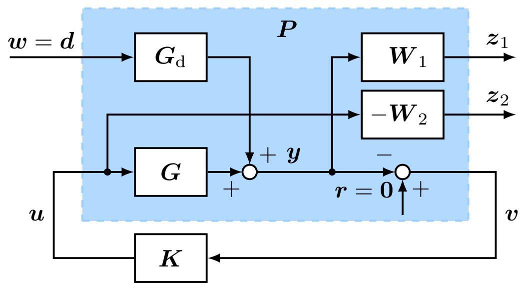

Figure 1. $\boldsymbol{SG}_\mathrm{d}/\boldsymbol{KSG}_\mathrm{d}$ mixed-sensitivity optimization

ing of optimization. Note that some curricula already provide this knowledge via mandatory courses.

3.3 Mixed-sensitivity $\mathcal{H}_\infty$ optimal control

Utilizing frequency-dependent weights, the sensitivity function $\boldsymbol{S} = (\mathbf{I} + \boldsymbol{GK})^{-1}$ is shaped along with other closed-loop transfer functions. The specific design is obtained by stacking these terms on top of each other in an overall closed-loop performance transfer function matrix $\boldsymbol{N}$ and minimizing its $\mathcal{H}_\infty$ norm with respect to an internally stabilizing controller $\boldsymbol{K}$:

$$\min_{\boldsymbol{K}} \|\boldsymbol{N}(\boldsymbol{K})\|_\infty \tag{7}$$

The design specifications are fulfilled (i.e. Nominal Performance (NP) is achieved) if ($\bar{\sigma}$ is the maximum singular value)

$$\|\boldsymbol{N}\|_\infty = \max_\omega \bar{\sigma}\left(\boldsymbol{N}(\mathrm{j}\omega)\right) < 1. \tag{8}$$

Figure 1 depicts the mixed-sensitivity $\mathcal{H}_\infty$ control problem for disturbance rejection. The exogenous input signal $\boldsymbol{w}$ entering the generalized plant $\boldsymbol{P}$ is the disturbance $\boldsymbol{d}$ and the control inputs are $\boldsymbol{u}$. The measured outputs $\boldsymbol{v}$ are fed back to the controller $\boldsymbol{K}(s)$. Utilizing a frequency-dependent performance weight $\boldsymbol{W}_1(s)$ and an input weight $\boldsymbol{W}_2(s)$, the exogenous output signal $\boldsymbol{z} = \left[\, \boldsymbol{z}_1^\mathrm{T} \; \boldsymbol{z}_2^\mathrm{T} \,\right]^\mathrm{T}$, where $\boldsymbol{z}_1 = \boldsymbol{W}_1\boldsymbol{y}$ and $\boldsymbol{z}_2 = -\boldsymbol{W}_2\boldsymbol{u}$ is defined and the generalized plant $\boldsymbol{P}$ is given by

$$\begin{bmatrix} \boldsymbol{z}_1 \\ \boldsymbol{z}_2 \\ \boldsymbol{v} \end{bmatrix} = \underbrace{\left[\begin{array}{c|c} \boldsymbol{W}_1\boldsymbol{G}_\mathrm{d} & \boldsymbol{W}_1\boldsymbol{G} \\ \mathbf{0} & -\boldsymbol{W}_2 \\ \hline -\boldsymbol{G}_\mathrm{d} & -\boldsymbol{G} \end{array}\right]}_{\boldsymbol{P}} \begin{bmatrix} \boldsymbol{w} \\ \boldsymbol{u} \end{bmatrix} \tag{9}$$

Closing the lower feedback loop with the controller $\boldsymbol{K}$ yields the closed-loop performance transfer function matrix $\boldsymbol{N}$:

$$\begin{bmatrix} \boldsymbol{z}_1 \\ \boldsymbol{z}_2 \end{bmatrix} = \underbrace{\begin{bmatrix} \boldsymbol{W}_1\boldsymbol{SG}_\mathrm{d} \\ \boldsymbol{W}_2\boldsymbol{KSG}_\mathrm{d} \end{bmatrix}}_{\boldsymbol{N}} \boldsymbol{w} \tag{10}$$

It can be shown that because $\boldsymbol{KS}$ is part of the stack in (10), the design is robustly stable with respect to (full complex) additive uncertainty $\boldsymbol{E}_\mathrm{A}(s) = \boldsymbol{G}_\mathrm{p}(s) - \boldsymbol{G}(s)$ (with a perturbed plant $\boldsymbol{G}_\mathrm{p}$) with $\bar{\sigma}\left(\boldsymbol{E}_\mathrm{A}(\mathrm{j}\omega)\right) < \frac{1}{\bar{\sigma}(\boldsymbol{KS}(\mathrm{j}\omega))}$ if (8) holds.

The students need knowledge of advanced linear algebra and of basics of frequency domain representations to understand the concepts of this design. Additionally, special training in the concept of singular values is essential. Such design methods are therefore typically taught in elective courses or advanced seminars.

3.4 DK synthesized μ-"optimal" control

The D(G)K-iteration (see Skogestad and Postlethwaite (2005)) is an algorithm to design a μ-(sub-)optimal controller that minimizes a given μ-condition for a general uncertainty structure utilizing a normalized, block-diagonal, linear time-invariant (LTI) perturbation matrix

$$\boldsymbol{\Delta} \in \boldsymbol{\Delta}_\mathrm{B} \;\Leftrightarrow\; \|\boldsymbol{\Delta}\|_\infty \leq 1,\ \boldsymbol{\Delta} \text{ LTI, structured, and stable.} \tag{11}$$

The choice of structure of the unknown but normalized perturbation block $\boldsymbol{\Delta}_i$ ($\|\boldsymbol{\Delta}_i\|_\infty \leq 1$) is crucial. Frequency dependent weights $\boldsymbol{W}_i(s)$ are utilized to shape the uncertainty over frequency.

If nominal stability (NS) of the design is fulfilled and the robust stability (RS) μ-value is less than one this corresponds to a stable closed-loop for all considered uncertainties. If additionally the robust performance (RP) μ-value is less than one, then also the formulated performance requirements are fulfilled in all these cases.

Figure 2 shows a system with multiplicative input and output uncertainties ("I", "O"), as well as additive uncertainty ("A"). The set of possible perturbed plants $\boldsymbol{G}_\mathrm{p}(s)$ ($m \times r$) around the nominal model $\boldsymbol{G}(s)$ ($m \times r$) is defined by

$$\boldsymbol{G}_\mathrm{p} = (\mathbf{I} + \boldsymbol{\Delta}_\mathrm{O}\boldsymbol{W}_{1\mathrm{O}})(\boldsymbol{G} + \boldsymbol{\Delta}_\mathrm{A}\boldsymbol{W}_{1\mathrm{A}})(\mathbf{I} + \boldsymbol{\Delta}_\mathrm{I}\boldsymbol{W}_{1\mathrm{I}}). \tag{12}$$

Thereby, $\mathbf{I}$ denotes the identity matrix, $\boldsymbol{\Delta}_\mathrm{I}(s)$ ($r \times r$) and $\boldsymbol{\Delta}_\mathrm{O}(s)$ ($m \times m$) are considered as unknown but norm-bounded ($\|\boldsymbol{\Delta}_\mathrm{I}\|_\infty \leq 1$ and $\|\boldsymbol{\Delta}_\mathrm{O}\|_\infty \leq 1$) complex diagonal matrices, i.e. no coupling between different input channels or output channels, respectively. This onset is commonly used to model actuator respectively sensor magnitude and phase uncertainty over frequency. In contrast, $\boldsymbol{\Delta}_\mathrm{A}(s)$ ($m \times r$) is considered as an unknown but norm-bounded ($\|\boldsymbol{\Delta}_\mathrm{A}\|_\infty \leq 1$) full complex perturbation matrix, where any coupling from its inputs to its outputs is possible, and phase relations are unknown.

The generalized plant $\boldsymbol{P}$, which is an open-loop system, is obtained by opening all "loops" before and after the controller $\boldsymbol{K}$. For the system in Figure 2 with inputs and outputs as evident from (13) $\boldsymbol{P}$ is given by (14).

$$\begin{bmatrix} \boldsymbol{y}_{\boldsymbol{\Delta}_\mathrm{I}} \\ \boldsymbol{y}_{\boldsymbol{\Delta}_\mathrm{A}} \\ \boldsymbol{y}_{\boldsymbol{\Delta}_\mathrm{O}} \\ \boldsymbol{z}_1 \\ \boldsymbol{z}_2 \\ \hline \boldsymbol{v} \end{bmatrix} = \underbrace{\left[\begin{array}{c|c} \boldsymbol{P}_{11} & \boldsymbol{P}_{12} \\ \hline \boldsymbol{P}_{21} & \boldsymbol{P}_{22} \end{array}\right]}_{\boldsymbol{P}} \begin{bmatrix} \boldsymbol{u}_{\boldsymbol{\Delta}_\mathrm{I}} \\ \boldsymbol{u}_{\boldsymbol{\Delta}_\mathrm{A}} \\ \boldsymbol{u}_{\boldsymbol{\Delta}_\mathrm{O}} \\ \boldsymbol{w} \\ \hline \boldsymbol{u} \end{bmatrix} \tag{13}$$

$$\boldsymbol{P} = \left[\begin{array}{cccc|c} \mathbf{0} & \mathbf{0} & \mathbf{0} & \mathbf{0} & \boldsymbol{W}_{1\mathrm{I}} \\ \boldsymbol{W}_{1\mathrm{A}} & \mathbf{0} & \mathbf{0} & \mathbf{0} & \boldsymbol{W}_{1\mathrm{A}} \\ \boldsymbol{W}_{1\mathrm{O}}\boldsymbol{G} & \boldsymbol{W}_{1\mathrm{O}} & \mathbf{0} & \mathbf{0} & \boldsymbol{W}_{1\mathrm{O}}\boldsymbol{G} \\ \boldsymbol{W}_\mathrm{P}\boldsymbol{G} & \boldsymbol{W}_\mathrm{P} & \boldsymbol{W}_\mathrm{P} & \boldsymbol{W}_\mathrm{P}\boldsymbol{G}_\mathrm{d} & \boldsymbol{W}_\mathrm{P}\boldsymbol{G} \\ \mathbf{0} & \mathbf{0} & \mathbf{0} & \mathbf{0} & \boldsymbol{W}_\mathrm{U} \\ \hline -\boldsymbol{G} & -\mathbf{I} & -\mathbf{I} & -\boldsymbol{G}_\mathrm{d} & -\boldsymbol{G} \end{array}\right] \tag{14}$$

By closing the lower feedback loop between $\boldsymbol{P}$ and $\boldsymbol{K}$ using a lower linear fractional transformation (LFT) the nominal closed-loop system $\boldsymbol{N}$ is derived:

$$\boldsymbol{N} = \mathcal{F}_\mathrm{l}(\boldsymbol{P}, \boldsymbol{K}) = \boldsymbol{P}_{11} + \boldsymbol{P}_{12}\boldsymbol{K}(\mathbf{I} - \boldsymbol{P}_{22}\boldsymbol{K})^{-1}\boldsymbol{P}_{21} \tag{15}$$

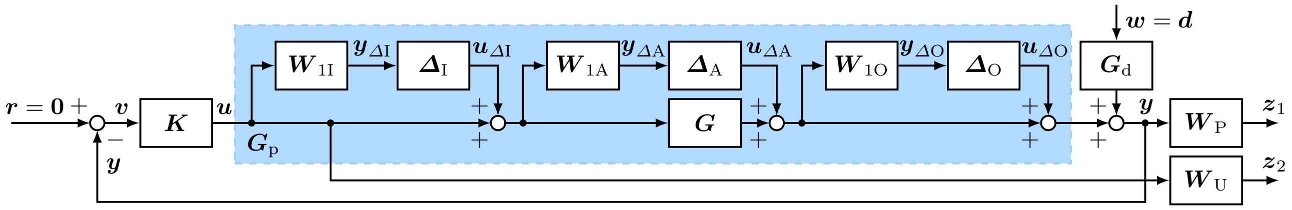

Figure 2. Augmented plant interconnection with uncertainties for DK-synthesized μ-"optimal" control design.

$$\begin{bmatrix} \boldsymbol{y}_{\boldsymbol{\Delta}_\mathrm{I}} \\ \boldsymbol{y}_{\boldsymbol{\Delta}_\mathrm{A}} \\ \boldsymbol{y}_{\boldsymbol{\Delta}_\mathrm{O}} \\ \hline \boldsymbol{z}_1 \\ \boldsymbol{z}_2 \end{bmatrix} = \underbrace{\begin{bmatrix} \boldsymbol{N}_{11} & \boldsymbol{N}_{12} \\ \boldsymbol{N}_{21} & \boldsymbol{N}_{22} \end{bmatrix}}_{\boldsymbol{N}} \begin{bmatrix} \boldsymbol{u}_{\boldsymbol{\Delta}_\mathrm{I}} \\ \boldsymbol{u}_{\boldsymbol{\Delta}_\mathrm{A}} \\ \boldsymbol{u}_{\boldsymbol{\Delta}_\mathrm{O}} \\ \hline \boldsymbol{w} \end{bmatrix} \qquad (16)$$

Alternatively, $\boldsymbol{N}$ can be derived directly from Figure 2 by evaluating the closed-loop transfer function from inputs to outputs as evident from (16) without opening the "loops" before and after the controller $\boldsymbol{K}$.

Information on DK-iteration and a precise definition of the control objectives in robust control is found in Skogestad and Postlethwaite (2005) and Zhou et al. (1996). Although the cited textbook is of high quality, the mathematical and implementation demands are high even for graduate students, and a successful design and implementation heavily depends on individual coaching.

4. FLEXIBLE BEAM

4.1 Laboratory setup

The experimental setup utilized in this work is a vertically mounted hinged-hinged structural bending beam shown schematically in Figure 3, see also Jovanova et al. (2013). On each side four MFC piezo patches are bonded to the beam. The piezo patches at the front operate as actuators, those at the back function as sensors (collocation).

Remark 1. Actuator/sensor placement affects the gains and zeros of the system plant. A configuration optimized for the first 4 bending modes has been found in the design of the test bed setup.

Although piezo actuators and sensors in principle do exhibit hysteresis behavior, this effect was not considered further in this work. It is justified to approximate the utilized MFCs via a linear gain because they show only minor nonlinearities, see Smart Material (2013). An electrodynamic shaker introduces a traversal disturbance force. MATLAB® and Simulink® were chosen as control engineering tools. The student developed the required functionality for controller design and system identification using standard MATLAB® toolboxes, the "robust control toolbox" and the "system identification toolbox". The controllers were realized and executed in real time via the dSPACE ACE 1104 platform.

In this work, the sophisticated experimental MIMO test bed of Figure 3 was already available. Its development and implementation had been carried out in previous student projects. This enabled a direct, frustration-free and efficient controller implementation and measurement data acquisition during the master work.

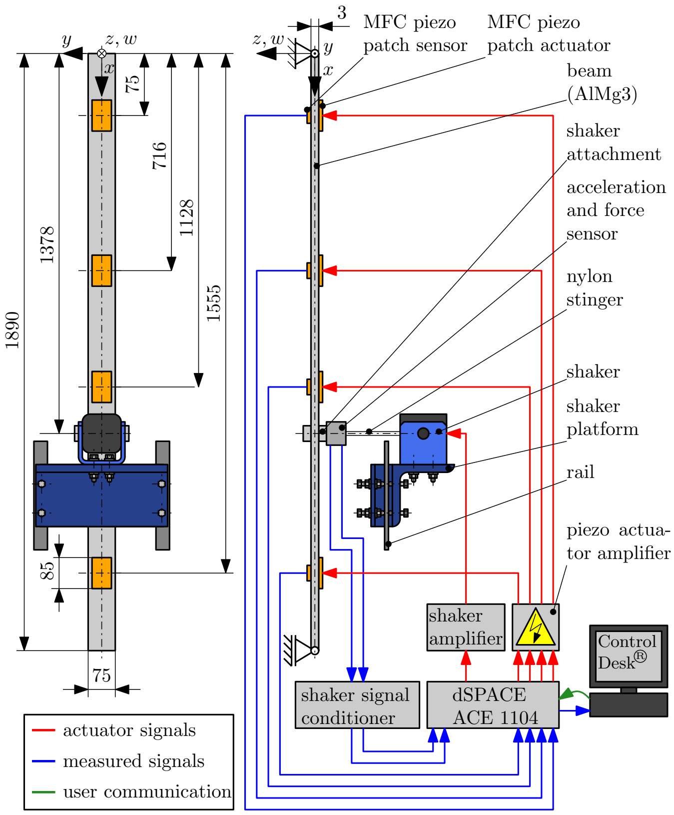

Figure 3. Schematic sketch of the experimental set-up

4.2 Identified (ID) Plant Model

In order to directly capture the physical couplings between inputs and outputs a MIMO identification procedure was used. Measurement data were filtered and down-sampled to 100 Hz. Mean values were subtracted and linear trends removed. Then the subspace algorithm N4SID (Overschee and Moor, 1996) of the MATLAB® System Identification Toolbox™ was applied to identify stable, linear state-space models in discrete-time.

The model which achieved the best model fit in a cross-validation was used for simulation purposes. An alternatively designed FE model of the beam revealed five structural modes below 50 Hz. By modally truncating real-valued poles a low-order model was obtained and used as design plant. This approach also enabled the quantification of model errors and their effects on stability and performance by investigating simulated control behavior. Moreover, this enabled the engineer to robustify the controller design by directly considering the model errors using DK-synthesized μ-"optimal" control.

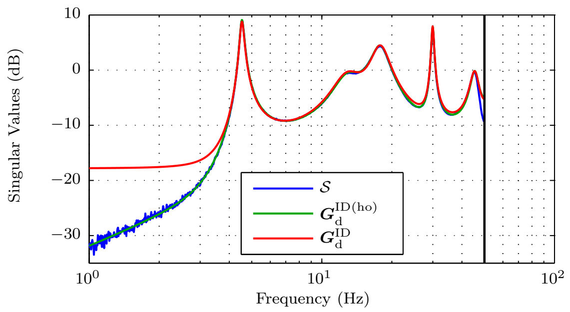

Figure 4. Singular values (disturbance model) for parametric and non-parametric ($\mathcal{S}$) identified models

Remark 2. The system dynamics are infinite dimensional. In Curtain and Zwart (1995) theory for control of infinite-dimensional systems is presented. In Bontsema et al. (1988) three partial differential equation models for a flexible beam (with different types of damping and varying parameter values) are obtained and robustly stabilized. However, the task in this work focuses on obtaining a finite-dimensional dynamic model and applying modern optimal and robust control design methods.

In Figure 4 the "ID(ho)" (high-order) and the "ID" (used for controller design) disturbance model are compared with the "$\mathcal{S}$ model", a non-parametric (identified), spectral model. Static deformation cannot be measured by the utilized sensors as evident in Figure 4 ("$\mathcal{S}$ model", "ID(ho)" at low frequencies). The reduced system ("ID") focuses on the modal dynamics and does not show this behavior. Within the frequency range of interest spanned by the natural frequencies of the first five structural modes (peaks) the models match well. As evident from Figure 4 the modes, particularly the first and fourth, are only weakly damped. Therefore, active damping of these lowest damped structural modes was defined as control task.

Note that knowledge on system identification requires stochastic fundamentals as well as specific courses on parameter estimation and measurement procedures.

5. CONTROL DESIGN

5.1 Modally weighted LQG design

Because $\boldsymbol{A}$ had complex-conjugate eigenvalues (i.e. complex-conjugate eigenvectors) the weighting factors m_i in $\boldsymbol{M}$ (17) were assigned in pairs. The first two diagonal elements of $\boldsymbol{M}$ were utilized for weighting the first structural mode, the next two diagonal elements of $\boldsymbol{M}$ for weighting the second structural mode, and so on. A high value m_i means that the corresponding eigenmode $\boldsymbol{s}_i$ is weighted strongly in the (modal) state weighting matrix $\boldsymbol{Q}$ (by m_i^2) and thus the improvement of damping of this eigenmode $\boldsymbol{s}_i$ is important in terms of the objective function (5):

$$\boldsymbol{M} = \mathrm{diag}\{120, 120, 30, 30, 50, 50, 100, 100, 50, 50\} \quad (17)$$

Because all four piezo patch actuators are identical, the input weighting matrix $\boldsymbol{R}$ was chosen as a matrix of diagonally repeated values, i.e. $\boldsymbol{R} = 2000 \cdot \mathbf{I}_{[4\times4]}$. Thus, inputs of the actuators are penalized equally. The covariance matrices $\boldsymbol{W}$ and $\boldsymbol{V}$ were chosen based on covariance information from identification data (see Dullinger (2013)).

5.2 Mixed-Sensitivity $\mathcal{H}_\infty$ design

The scalar performance weight $W_1(z)$ was chosen as a band-pass. Extra peaks were utilized to put strong weight on the low-damped first and fourth modes. Thus, by design of $W_1(z)$, performance was not an issue at low and high frequencies, where actuation was not desired with the applied piezo patch actuators, respectively where the system is simply unknown. The scalar input weight $W_2(z)$ was selected as a band-stop, thus inputs were highly penalized outside the frequency range of interest.

The dynamics of the performance and input weights, $W_1(z) = k_1 \cdot \breve{W}_1(z)$ respectively $W_2(z) = k_2 \cdot \breve{W}_2(z)$ were chosen based on closed-loop simulations on the "ID(ho)"-model. Then, a variety of designs was derived by changing only the constant gain k_2 of $W_2(z)$. Subsequently, a data set for that design with the smallest value of k_2 which achieved stability in the experiment was recorded and evaluated.

Although uncertainty is not explicitly modelled by this mixed-sensitivity $\mathcal{H}_\infty$ design, it is robustly stable for all perturbed plants $\boldsymbol{G}_{\mathrm{p}}$ with

$$\bar{\sigma}\left(\boldsymbol{G}_{\mathrm{p}}(\mathrm{e}^{\mathrm{j}\omega T_{\mathrm{s}}}) - \boldsymbol{G}(\mathrm{e}^{\mathrm{j}\omega T_{\mathrm{s}}})\right) \leq \left|W_{1\mathrm{A}}(\mathrm{e}^{\mathrm{j}\omega T_{\mathrm{s}}})\right| \quad \forall \omega \in \mathbb{R} \quad (18)$$

where $\left|W_{1\mathrm{A}}(\mathrm{e}^{\mathrm{j}\omega T_{\mathrm{s}}})\right| = \frac{(1-\epsilon)}{\bar{\sigma}(\boldsymbol{KS}(\mathrm{e}^{\mathrm{j}\omega T_{\mathrm{s}}}))}$ with an infinitesimally small $\epsilon \in \mathbb{R}^+$.

5.3 DK synthesized μ-"optimal" design

Here, the performance weight $\boldsymbol{W}_{\mathrm{P}}(z)$ and input weight $\boldsymbol{W}_{\mathrm{u}}(z)$ were chosen in a similar fashion as for the Mixed-Sensitivity $\mathcal{H}_\infty$ design (see Fig. 5). The uncertainty weights $W_{1\mathrm{I}}(s)$ and $W_{1\mathrm{O}}(s)$ for complex diagonal multiplicative input/output uncertainty were chosen as scalar band-stop filters. At those low and high frequencies where the uncertainty weights $W_{1\mathrm{I}}(s)$ and $W_{1\mathrm{O}}(s)$ exceed 0 dB, the design allows for more than 100 % multiplicative (input respectively output) uncertainty. Consequently, the phase of each SISO transfer function representing a physical system on the plant's input respectively output side is considered unknown.

For the additive uncertainty weight $W_{1\mathrm{A}}(z)$ the following approach was taken. Let the set of plants Π represented by additive uncertainty contain the perturbed plants

$$\boldsymbol{G}_{\mathrm{p}} = \boldsymbol{G} + \underbrace{W_{1\mathrm{A}}\boldsymbol{\Delta}_{\mathrm{A}}}_{\boldsymbol{E}_{\mathrm{A}}} \quad (19)$$

where $\boldsymbol{\Delta}_{\mathrm{A}}$ is a full complex norm-bounded perturbation ($\|\boldsymbol{\Delta}_{\mathrm{A}}\|_\infty \leq 1$) and where the scalar weight $W_{1\mathrm{A}}(z)$ is chosen such that at each frequency ω

$$\left|W_{1\mathrm{A}}(\mathrm{e}^{\mathrm{j}\omega T_{\mathrm{s}}})\right| \geq l_{\mathrm{A}}(\omega) \ \ \forall \omega \in \mathbb{R} \quad (20)$$

holds. Then, at each frequency ω the smallest scalar $l_{\mathrm{A}}(\omega)$ is given by

$$l_{\mathrm{A}}(\omega) = \max_{\boldsymbol{G}_{\mathrm{p}} \in \Pi} \bar{\sigma}(\underbrace{\boldsymbol{G}_{\mathrm{p}}(\mathrm{e}^{\mathrm{j}\omega T_{\mathrm{s}}}) - \boldsymbol{G}(\mathrm{e}^{\mathrm{j}\omega T_{\mathrm{s}}})}_{\boldsymbol{E}_{\mathrm{A}}(\mathrm{e}^{\mathrm{j}\omega T_{\mathrm{s}}})}). \quad (21)$$

Subsequently, $\boldsymbol{G}^{\mathrm{ID(ho)}}(z)$ was considered as one perturbed plant in (21), thus

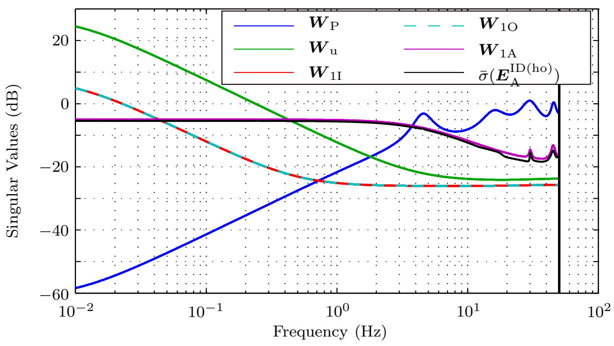

Figure 5. Singular values of scalar weights

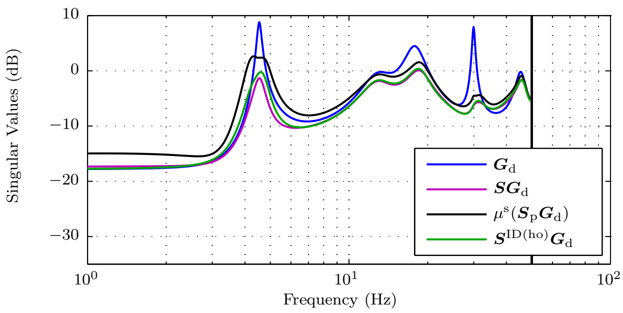

Figure 6. Simulated open-loop and closed-loop disturbance behavior

$$l_A(\omega) = l_A^{ID(ho)}(\omega) = \bar{\sigma}(\underbrace{G^{ID(ho)}(e^{j\omega T_s}) - G^{ID}(e^{j\omega T_s})}_{E_A^{ID(ho)}(e^{j\omega T_s})}). \quad (22)$$

holds. Then a simplified scalar rational weight $W_{1A}(z)$ was shaped so that at each frequency ω the magnitude of $W_{1A}(e^{j\omega T_s})$ was larger than $l_A^{ID(ho)}(\omega)$. This way, the chosen shape of $W_{1A}(z)$ accounted for the neglected dynamics of $G^{ID(ho)}(z)$. Figure 6 shows the open-loop and closed-loop singular values on the nominal model (G_d respectively SG_d), the worst-case gain of the closed-loop disturbance path ($\mu^s(S_pG_d(e^{j\omega T_s}))$, called the skewed-$\mu$-value, see Skogestad and Postlethwaite (2005)) and the closed-loop disturbance performance with the plant $G^{ID(ho)}(z)$ ($S^{ID(ho)}G_d$). As ensured by the fact that the design achieves robust stability (RS), applying the controller $K(z)$ on the particular perturbed plant $G^{ID(ho)}(z)$ results in a closed-loop stable system. Furthermore, the fact that the design accounts for the neglected dynamics of $G^{ID(ho)}(z)$ through additive uncertainty ensures that at a given frequency $\bar{\sigma}(S^{ID(ho)}G_d(e^{j\omega T_s})) < \mu^s(S_pG_d(e^{j\omega T_s}))$ holds, where $S^{ID(ho)} = (\mathbf{I} + G^{ID(ho)}K)^{-1}$.

6. EXPERIMENTAL RESULTS

The controllers designed in Sections 5.1 to 5.3 were implemented on the dSPACE platform and validated on the test bed. In order to obtain comparable results the same discrete white noise signal was applied as disturbance signal d. In Figure 7 the experimental results are compared in terms of singular values of spectral, non-parametric models (from d to y) using built-in MATLAB® functions.

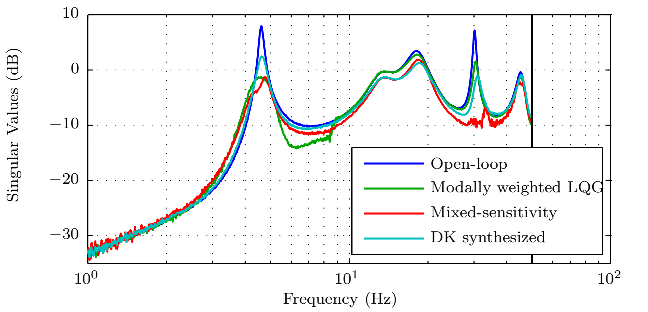

Figure 7. Experimental validated (disturbance rejection) performance in terms of singular values of identified spectral models ($d \rightarrow y$); design plant: ID model

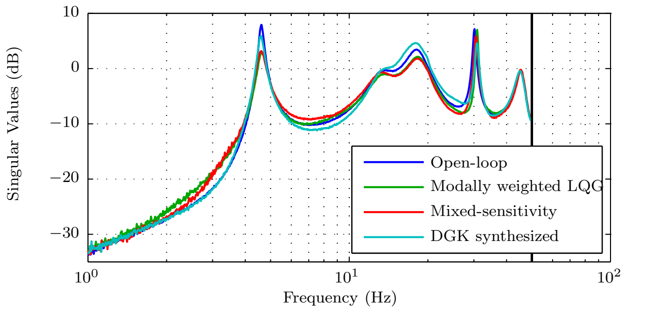

Figure 8. Experimental validated (disturbance rejection) performance in terms of singular values of identified spectral models ($d \rightarrow y$); design plant: FE model

It is evident that the LQG controller with modal weighting is well-suited to address the damping of the structural modes. However, the mixed-sensitivity $\mathcal{H}_\infty$ controller is clearly superior.

In principle it is possible to obtain the presented mixed-sensitivity $\mathcal{H}_\infty$ controller by the DK synthesized μ-"optimal" design method. Thus, the fact that the presented DK synthesized controller performs mostly inferior means that the modelled uncertainty (and/or performance weight) was chosen conservatively. Especially the additive uncertainty model which accounts for the neglected dynamics of $G^{ID(ho)}(z)$ limits control authority and performance.

An alternative dynamic model of the flexible beam was obtained by utilizing the FE method, see Dullinger (2013). For the FE model the natural frequency of the lowest-damped, fourth mode showed a large deviation (when comparing it to the presumably more accurate identified model). This critical model error lead to difficulties when designing controllers based on the FE model. This challenging control task was best accomplished by a DGK-synthesized controller with specific, tedious uncertainty tuning for that mode. Figure 8 presents the achieved results of the FE-model-based controllers. The LQG controller failed in this task, and the mixed-sensitivity $\mathcal{H}_\infty$ controller could only achieve a marginal improvement in damping.

7. CONCLUSIONS

In this work Linear-Quadratic Gaussian (LQG) control and optimal and robust $\mathcal{H}_\infty$ control design methods were investigated to achieve attenuation of the structural modes of a flexible beam. LQG control with modal weighting quickly produced useful results, and mixed-sensitivity $\mathcal{H}_\infty$ control was most appropriate in terms of performance and design effort. The potentially powerful D(G)K-synthesized μ-"optimal" design method requires considerable design effort which was only justified in special cases – to specifically tune control performance in the presence of large uncertainties of the FE model utilized as design plant.

LQG control (with modal weighting) contributes to the understanding of the principle of optimization by minimizing an objective function of weighted quantities. This provides a solid basis for $\mathcal{H}_\infty$ control and should therefore be part of mandatory control courses.

Mixed-sensitivity $\mathcal{H}_\infty$ control is ideal for getting started with $\mathcal{H}_\infty$ control. Its structure, i.e. the generalized plant $\boldsymbol{P}$ respectively the closed-loop performance transfer function matrix $\boldsymbol{N}$ is relatively simple to understand and the concept of closed-loop transfer function shaping by utilizing frequency-dependent weights can be studied. The tuning effort is kept within reasonable limits, and because of its robustness properties mixed-sensitivity $\mathcal{H}_\infty$ control enables a first glance at robust control without the requirement of a full μ-synthesis. It is quite realistic to teach this design in elective courses for master students of engineering curricula as the additional mathematical knowledge is manageable.

For a DK-synthesized design the recommendation is to start simple using only a few and only complex-valued uncertainty descriptions first. Then, in case of a continuous-time plant one can also think of including a parametric uncertainty description. Thereby, a modal form might facilitate its implementation and reduce the computational load. However, due to the overall complexity of this design, a successful design and implementation can only be expected from motivated master students.

Finally, the implementation on a test bed calls for a tried setup with a simple and fast control implementation by means of a user-friendly interface. This minimizes the overhead for test runs and boosts the students' motivation.

REFERENCES

(2011). VUT curriculum. `http://www.tuwien.ac.at/dekanate/mwb/studienplaene/`.

Athans, M. (1971). The role and use of the stochastic linear-quadratic-Gaussian problem in control system design. *Automatic Control, IEEE Transactions on*, 16(6), 529–552.

Bontsema, J., Curtain, R., and Schumacher, J. (1988). Robust control of flexible structures a case study. *Automatica*, 24, 177186.

Curtain, R.F. and Zwart, H. (1995). *An Introduction to Infinite-Dimensional Linear Systems Theory*. Springer.

Dullinger, C. (2013). *Comparison of optimal and robust MIMO control concepts for active vibration damping of a flexible beam laboratory setup*. Master's thesis, TU Vienna.

Gawronski, W.K. (2004). *Advanced Structural Dynamics an Active Control of Structures*. Springer.

Jovanova, J., Gavriloski, V., Schirrer, A., and Kozek, M. (2013). Multidisciplinary laboratory experiment for active vibration control with piezoelectric patches. In *Global Engineering Education Conference (EDUCON), 2013 IEEE*, 1093–1097. doi:10.1109/EduCon.2013.6530244.

Kheir, N., Åström, K.J., Auslander, D., Cheok, K.C., Franklin, G.F., Masten, M., and Rabins, M. (1996). Control systems engineering education. *Automatica*, 32(2), 147–166.

Kozek, M., Görtler, G., and Jörgl, H.P. (1999). MRACLab - a tool for teaching model reference adaptive control. In *Proceedings 14th IFAC World Congress 1999*.

Overschee, P.v. and Moor, B. (1996). *Subspace Identification for Linear Systems: Theory - Implementation - Applications*. Kluwer Academic Publishers.

Schirrer, A. (2011). *Efficient robust control design and optimization methods for flight control*. Ph.D. thesis, Vienna University of Technology, Vienna.

Senol, B., Yeroglu, C., and Erturkler, M. (2012). Development of a user friendly toolbox for advanced control education. *Fractional Differentiation and its Applications*.

Skogestad, S. and Postlethwaite, I. (2005). *Multivariable Feedback Control*. Wiley.

Smart Material (2013). Macro Fiber Composite - MFC. `http://www.smart-material.com/MFC-product-main.html`.

Ye, Z., Mohamadian, H., Yin, H., Zhang, G., and Pang, S. (2009). Advancing laboratory education in control engineering with practical implementation approaches. *WSEAS Transactions on Advances in Engineering Education*, 6(2), 55–65.

Zhou, K., Doyle, J.C., and Glover, K. (1996). *Robust and optimal control*. Prentice Hall (Upper Saddle River, NJ).